Proceedings of the 32nd European Safety and Reliability Conference (ESREL 2022)
Edited by Maria Chiara Leva, Edoardo Patelli, Luca Podofillini, and Simon Wilson
 Published by Research Publishing, Singapore.
doi: 10.3850/978-981-18-5183-4_S03-03-221-cd

Comparative assessment of models of cascading failures in power networks under seismic hazard

Hugo Rosero-Velásquez
Engineering Risk Analysis Group, TU-München, Germany. E-mail: hugo.rosero@tum.de

Juan Camilo Gómez-Zapata
Seismic Hazard and Risk Dynamics, Helmholtz Centre Potsdam German Research Centre for Geosciences GFZ & Institute for Geosciences, University of Potsdam, Germany. E-mail: jcgomez@gfz-potsdam.de

Daniel Straub
Engineering Risk Analysis Group, TU-München, Germany. E-mail: straub@tum.de

Risk analysis of power networks under natural hazards requires a model of the power flow following initial failures in the network caused by the hazard. The model should include cascading failures through the network, for which different models have been proposed in the literature. Past studies have compared widely used models for assessing the performance of power networks, such as the topological, betweenness-based and power flow models, and found correlations among the model outcomes. However, they do not compare them for systems subjected to natural hazards, where other factors (e.g., seismic intensity and resulting ground motions) also affect the system performance. Ultimately, the choice of the appropriate model depends on the analysis purposes, the type of power network (e.g., transmission vs. distribution), the available amount of information, and computing resources. In this contribution, we investigate the effect of the cascading failure model on a seismic risk evaluation. To this end, we perform numerical investigations on the power network in the central coastal area of Valparaíso Region, Chile. Specifically, we compute and compare loss-exceedance functions for two models: Origin-destination betweenness centrality (ODBCM) and DC linear power flow (DCLPFM), for different representative seismic scenarios. We also compare the models with and without considering the uncertainty in the ground motion field.

Keywords: Cascading failures, critical infrastructure, uncertainty quantification, natural hazards, model selection

1. Introduction

Cascading failures in power networks are sequences of failure events that are triggered by local component failures. They depend on the network topology, the component capacities and the load redistribution. In the case of seismic hazards, the locations of the initial component failures depend on the seismic intensity and the components fragilities (Poljanšek et al., 2011; Ferrario et al., 2019).

Seismic risk assessment is associated with multiple uncertainties (Cornell, 1968; Moehle and Deierlein, 2004; Yang et al., 2009). One of them is the uncertainty in the model of cascading network failures. In this paper, we study the influence of the choice of the cascading failure model of power networks on the risk evaluation. We perform numerical investigations on the power network in the coastal area around Great Valparaíso, Chile.

2. Probabilistic seismic analysis for power networks

We follow the probabilistic hazard analysis framework of Fig. 1. We employ it for a probabilistic seismic hazard analysis of a power network, conditional on a hazard scenario. A similar framework can be found in (Moehle and Deierlein, 2004; Yang et al., 2009).

A seismic scenario is described with hazard parameters $\boldsymbol{\theta}$, such as magnitude, hypocentral location (i.e., longitude, latitude, depth) and orientation (i.e., rake, dip and strike angles). They are inputs for predicting the intensity measure $\mathbf{IM}$, at the location of power network components, such as power plants and substations. In seismic hazard analysis, $\mathbf{IM}$ corresponds to the ground motion

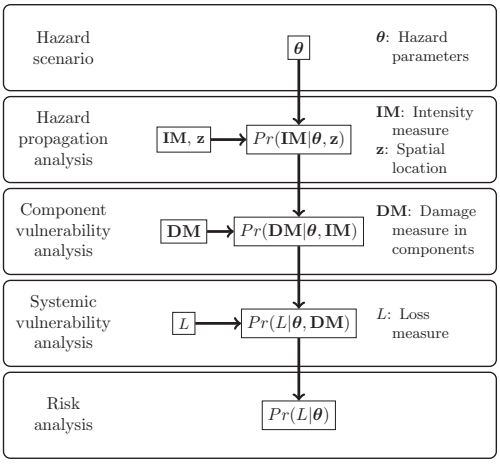

Fig. 1. Probabilistic hazard analysis, applicable to power networks (modified from Rosero-Velásquez and Straub, 2022)

field (GMF), e.g., the Peak Ground Acceleration (PGA), and multiple models for predicting GMF are available in the literature (Douglas, 2021). For considering the uncertainty in the prediction due to site effects, GMF prediction models can incorporate random fields (Wang and Takada, 2005; Jayaram and Baker, 2010).

The intensity measure is the input for evaluating the damage state of the power network components $\mathbf{DM}$, using fragility functions. A fragility function is a conditional probability distribution of the component damage state, given a intensity value. For simplicity, we consider binary component damage states, i.e., either "failure" or "no failure". Such fragility functions are available in the literature based on the components' functionality and power capacity (FEMA, 2003; Pitilakis et al., 2014).

We take the affected population as loss measure L. Based on census data and the power network topology, we divide the study area into consumption areas, and evaluate the population living in areas not reachable through the damaged network after cascading effects.

We evaluate the seismic scenario with Monte Carlo sampling of $\mathbf{IM}$ and $\mathbf{DM}$. The output is the conditional CDF of the affected population, or equivalently, its conditional loss-exceedance function.

3. Models of cascading failures

Power networks can be represented as weighted graphs. The nodes represent bars and generators, the edges correspond to lines and transformers, and the weights are associated with a physical property such as reactance. The topology can be derived combining GIS data and one-line diagrams.

Different models for simulating cascading failures are available in the literature (Crucitti et al., 2004; Farina et al., 2008; Hernández-Fajardo and Dueñas-Osorio, 2013). Here, we consider two models: the origin-destination betweenness centrality model (ODBCM), based on (Crucitti et al., 2004), and the DC linear power-flow model (DCLPFM), following (Farina et al., 2008). Comparisons between these models have already been performed in (Ouyang, 2013; Cupac et al., 2013; Abedi et al., 2019), but not in the context of a natural hazard risk assessment, which is the focus of our investigation.

We simulate the cascading failures as follows: First, we generate initial failures at the nodes. We do that by modelling $\mathbf{DM}$ at each node with a Bernoulli process, whose probability of failure is conditional on $\mathbf{IM}$ and defined by the nodal component fragility function, as shown in Fig. 1. Then we simulate the system response without the failed components. The response is a load redistribution among the surviving components, and for some of them the new load might exceed their capacity. If that occurs at a node or edge, then it fails too. We repeat these steps (i.e., simulating system response without failed components and identifying new component failures) until no new failure occurs. Finally, we evaluate the affected population, i.e., the total the population in the disconnected consumption areas.

A common assumption is to set component capacities proportional to the component load in the undamaged network, using a tolerance factor $\alpha \geq 1$ (Crucitti et al., 2004; Ouyang, 2013). $\alpha \to 1$ implies that the power grid operates close to its limit capacity and cascading failures will occur with a probability approaching one. With

$\alpha \geq 2.0$, the grid operates far below component capacities and becomes robust against cascading failures. Based on the reviewed literature, we set $\alpha = 1.2$.

3.1. *Origin-destination betweenness centrality model (ODBCM)*

This models computes the load $L_i(\mathbf{dm})$ at component i, given the damage state of the power network components $\mathbf{dm}$, as proportional to its origin-destination betweenness centrality:

$$L_i(\mathbf{d}) \propto \frac{1}{|\mathcal{S}||\mathcal{T}|} \sum_{\substack{s \in \mathcal{S} \\ t \in \mathcal{T} \\ s \neq t}} \frac{r_{sit}(\mathbf{dm})}{r_{st}(\mathbf{dm})} \tag{1}$$

$\mathcal{S}$ and $\mathcal{T}$ are the sets of source and terminal nodes, respectively; $|\cdot|$ is the cardinality operator; $r_{st}(\mathbf{dm})$ is the number of shortest paths connecting nodes s and t, given $\mathbf{dm}$; and $r_{sit}(\mathbf{dm})$ is the number of shortest paths connecting s and t and passing through component i, also given $\mathbf{dm}$. Eq. (1) is applicable to nodes and edges as components. We employ an adapted version of the algorithm proposed in (Brandes, 2001) for computing the betweenness centrality, which is available in the Python package Networkx.

Goh et al. (2001) have studied the betweenness centrality for computing network loads in scale-free networks. It has been applied to represent power networks (Crucitti et al., 2004; Hernández-Fajardo and Dueñas-Osorio, 2013).

The ODBCM requires only basic information about the power network (e.g., topology and line reactance), and the computational cost is lower than DCLPFM. However, it does not consider the power demand. Therefore, power specific risk metrics such as energy not supplied are not possible to obtain directly through ODBCM.

3.2. *DC linear power flow model (DCLPFM)*

The load $L_i(\mathbf{dm})$ at bus i given the damage state of the power network components $\mathbf{dm}$ is the power calculated from the power flow equations (El-Hawary, 2008)

$$s_i(\mathbf{dm}) = v_i(\mathbf{dm}) \sum_k \left(y_{ik}(\mathbf{dm})\right)^* \left(v_k(\,\mathbf{dm})\right)^* \tag{2}$$

The unknown $s_i = p_i + \imath q_i$ is the power at bus i, wherein p_i and q_i are real and reactive power, respectively; the unknown $v_k = |v_k| \exp(\imath\theta_k)$ is the voltage at node k; and the known quantity $y_{ik} = g_{ik} + \imath b_{ik}$ is the complex admittance between buses i and k ($\imath^2 = -1$). For simplicity, we neglect their dependence on $\mathbf{dm}$. At each bus two out of the four variables (i.e. p_i, q_i, $|v_k|$ or θ_k) are known.

The behavior of high voltage transmission networks in stationary regime can be described by linearizing Eq. (2), under three assumptions (Farina et al., 2008): the resistance is much smaller than the reactance, ($g_{ik} << b_{ik}$); the difference $\theta_{ik} = \theta_i - \theta_k$ in the voltage angles is small; and the voltage magnitudes are approximately equal to a base voltage ($|v_k| \approx 1$ in proper-unit system). Under these assumptions, the power can be expressed as a real quantity, and Eq. (2) results in:

$$s_i = p_i = \sum_k b_{ij}\theta_{ik} \tag{3}$$

Eq. (3) is also used for finding initial guesses to solve Eq. (2) with iterative solvers such as Gauss-Seidel and Newton-Raphson (El-Hawary, 2008).

We employ the Python software PyPSA (Brown et al., 2018) for solving Eq. (3). The required input are the line and transformer reactances, and the loads at buses and generators. The output includes the power flow through the lines, buses and transformers. This output is the load $L_i(\mathbf{dm})$ utilized for detecting overloaded components during the cascading effects simulation.

Typically, only the load demand at the buses is known, and the loads at the generators, which balance the load demands, are computed by minimizing the generation costs, which is the so-called DC optimal power flow model (Ferrario et al., 2019). However, in this work we take the load demand and generation from historical records.

Unlike ODBCM, DCLPFM considers the demand, and computes the loads in terms of power, which allows to evaluate the risk not only in terms

of affected population, but also in terms of power loss. We note that DCLPFM models are still a strong idealization of the real behaviour. Firstly, they model the stationary regime of the network, which is not expected during cascading failures. Secondly, they do not optimize the power flow when a component is removed, which can cause unrealistic overloads during balancing.

4. Numerical investigations

We study the influence of the choice of the cascading failure model on the population affected by a power network failure in the central coastal area of Valparaíso Region, Chile.

The study area is located in central Chile, with geographical extent as shown in Fig. 2. We delimited the consumption areas, based on the existing distribution lines. Based on the latest Chilean Census (INE, 2017), the consumption areas host around 1.38×10^6 inhabitants.

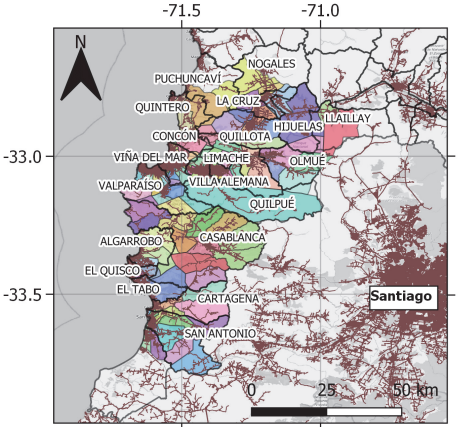

Fig. 2. Consumption areas in study area, based on distribution lines, provided in 2018 by the Superintendency of Oil and Electricity (SEC). Labels in upper case are the communes of the 5th Region of Valparaíso that are covered by the study area. Basemap: OpenStreetMap

Fig. 3 shows the power network model. It considers the high voltage lines (bright red thick lines) connecting Gran Valparaíso with the National Electric System (SEN) (dark red lines) (CNE, 2016; Coordinador, 2019). The straight orange lines simplify the distribution lines (see Fig. 2).

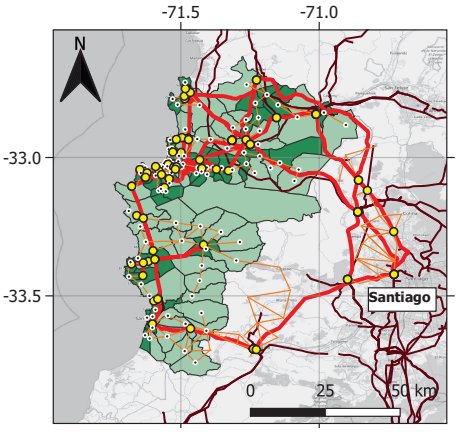

Fig. 3. Power network model for the study area. The consumption areas are colored by population density, in people per km^2, with ranges of $0-100$ (light green) and $100 - 11400$ (dark green). Basemap: OpenStreetMap

4.1. *Hazard scenarios*

Chile is highly exposed to extreme seismic events. Historical events include the 1960 seismic event with magnitude $M_w = 9.5$ in Valdivia, the 1985 event with $M_w = 8.0$ in Algarrobo, and the 2010 event with $M_w = 8.8$ in the Maule Region (Tang and Eidinger, 2006; CSN, 2022). Different studies have derived site specific ground motion models (Montalva et al., 2017; Hussain et al., 2020). Based on a stochastic catalogue obtained with the event-based calculator of OpenQuake (GEM, 2022), we selected four seismic scenarios. The hazard parameters are shown in Tab. 1 and epicentre locations in Fig. 4. In this study, we exclude the tsunami damages in Scenarios 18489 and 542.

The stochastic catalogue provides 20 random GMF realizations per scenario in terms of PGA, using a spatial correlation model proposed in (Jayaram and Baker, 2009).

4.2. *Power network vulnerability model*

We assign fragility functions to substations and power plants according to (FEMA, 2003), classifying them into three categories: medium-voltage substation, low-voltage substation, and medium/large generation plants. All of them have anchored components. Table 2 shows the fragility

Table 1. Hazard parameters of the selected seismic scenarios for the comparative assessment.

Scenario	6285	1401	18489	542
Mag.	6.15	7.15	8.05	9.35
Lon.[°]	-70.89	-70.92	-71.53	-74.02
Lat. [°]	-32.93	-32.93	-32.80	-39.32
Depth[km]	5.00	12.60	43.88	37.60
Rake [°]	90.00	90.00	90.00	90.00
Dip [°]	45.00	45.00	10.92	18.31
Strike [°]	0.02	0.07	9.90	9.73

Notes: Computed with OpenQuake (GEM, 2022). The catalogue has around 23000 scenarios with $M_w \geq 6.0$

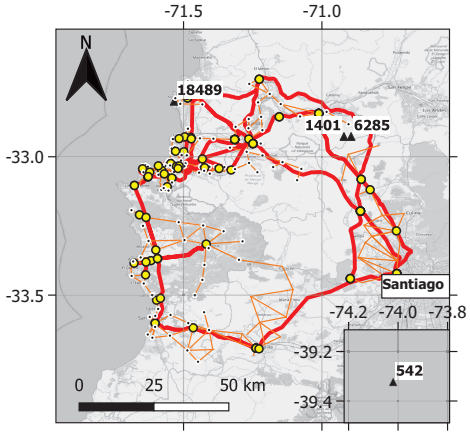

Fig. 4. Epicentre locations of the studied earthquake scenarios. Basemap: OpenStreetMap

function parameters for each category, representing an extensive damage state.

Table 2. Lognormal fragility parameters μ and σ for power network components under seismic hazard, for PGA in g (extensive damage state, all with anchored components)

Category	μ	σ
Medium-voltage substation	-1.05	0.40
Low-voltage substation	-1.61	0.35
Medium/large generation plant	-0.65	0.55

Source : FEMA (2003)

We construct the network model based on the one-line diagram and the geographic information of the SEN (Coordinador, 2019). Only the transmission components (big yellow dots and thick red lines in Fig. 3 and 4) are considered for simulating cascading effects.

For the loads in the DCLPFM, we took the hourly power generation and measurements from (Coordinador, 2019), corresponding to the day of maximum power generation in 2017, i.e. 28.12.2017. We assign randomly one of these hours to each of the cascading effect simulations, to represent the uncertainty in the loads.

4.3. *Results*

Firstly, we analyze a single simulation of cascading effects with both models. Fig. 5 shows the results for a random realization of initial component failures with the median GMF based on the GMF realizations, and with one random GMF, for Scenario 1401 ($M_w = 7.15$). One can observe that the random realization of the GMF amplifies the PGA in the most densely populated areas, hence increases the failure probabilities of most of the components. As a consequence, this random GMF also produces more initial random component failures than the median GMF and results in a larger affected population.

Secondly, Tab. 3 shows for all considered scenarios the average affected population evaluated with the two models, as well as their coefficient of variation and correlation coefficients between the outcomes of the two models. The statistics are based on 1000 Monte Carlo samples of initial failures, from which we compute the affected population with ODBCM and with DCLPFM. We compute the random initial failures with the median GMF, and with random GMFs.

Fig. 6 shows the conditional distribution of the affected population given the scenarios, as well as the scatter plots. One can observe that extreme impact events are more likely to occur with random GMF. Furthermore, the two cascading effect models disagree in the shape of the distribution tail in the simulations with the median GMF. In the scatter plots, one can observe that DCLPFM predicts a larger or equal affected population than ODBCM; with random GMF the difference can

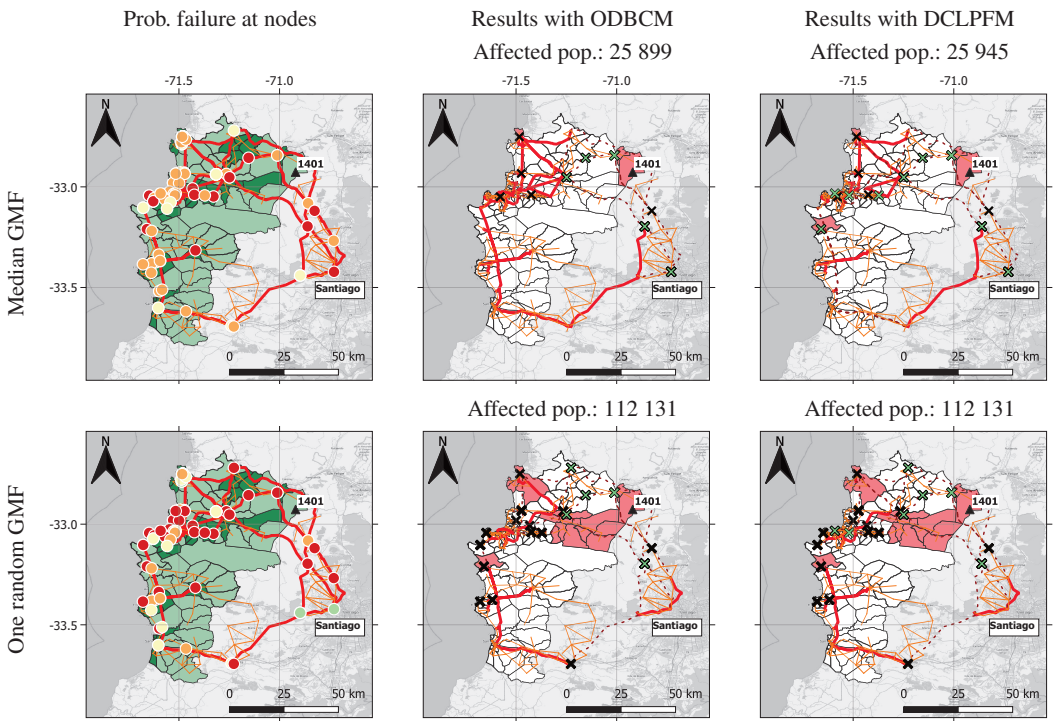

Fig. 5. Cascading effect simulation with the median GMF (upper row) and one random GMF (lower row) for Scenario 1401 ($M_w = 7.15$, black triangle). The left column shows failure probabilities at nodes, with green dots corresponding to a value below 10^{-4}, yellow between 10^{-4} and 10^{-2}, orange between 10^{-2} and 10^{-1}, and red dots larger than 10^{-1}. The areas in the left column are colored by density as in Fig. 3; the middle and right column show the results. Initial random failures are the black crosses in the maps, failures by cascading effects are represented by green crosses and dashed lines, and affected areas in the middle and right column are shown in red.

Table 3. Average affected population ODBCM vs. DCLPFM (in thousands), coefficient of variation (in brackets), and correlation coefficient ρ between the outcomes of the two models.

Scenario	Median GMF			Random GMF		
	ODBC	DCLPF	ρ	ODBC	DCLPF	ρ
6285	8.3	14.2	0.6	82.6	100.2	0.9
	(1.9)	(1.7)		(2.3)	(2.0)	
1401	22.0	38.4	0.4	101.5	125.9	0.8
	(1.2)	(1.6)		(1.6)	(1.6)	
18489	18.3	34.8	0.8	138.2	151.1	1.0
	(3.4)	(2.3)		(1.6)	(1.5)	
542	17.0	27.3	0.8	179.7	191.7	0.9
	(2.3)	(1.7)		(1.4)	(1.3)	

be up to a factor of 10. This can be explained by the power flow equations balancing, which is not present in ODBCM.

5. Concluding remarks

In this paper, we analyze the influence of the choice of cascading effects model on the resulting loss measure in the context of probabilistic seismic hazard analysis of power networks. We investigate the power network at the coastal area of Valparaíso, Chile, subjected to four selected seismic scenarios, taking the affected population as risk metric.

We compare two models: ODBCM and DCLPFM. Both models are cheap to compute, wherein ODBCM is faster and requires less input data than DCLPFM. In contrast, DCLPFM takes into account the load demand, and can be extended to more complex (and computationally more expensive) models, such as AC power flow

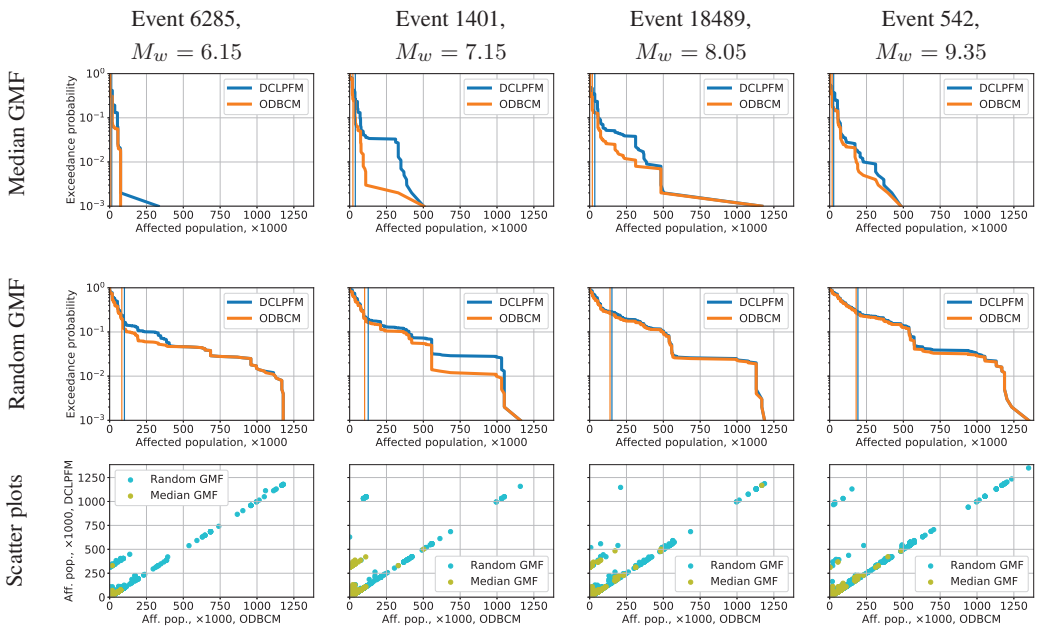

Fig. 6. Loss exceedance functions obtained with DCLPFM and ODBCM for different seismic scenarios (columns), Median (first row) and Random (second row) GMF. Vertical lines indicate the location of the sample average. The third row shows the scatter plots of the affected population, computed with ODBCM and DCLPFM.

model and optimal power-flow.

In the numerical investigations, assuming the same initial component failures, the two models can result in different cascading failures. The affected population calculated with DCLPFM is found to be either equal or larger than the one obtained with ODBCM. However, as shown in Fig. 6, the difference between the conditional means of the affected population between the two models is small. Load balancing of the power-flow equations can overestimate the power flow in the surviving components, and produce more severe cascading failures, as well as heavier tails in the conditional distribution, and slightly larger conditional mean, of the affected population. Further investigations for incorporating load balancing in ODBCM can consider either to reduce the tolerance factor α, or to assign weights to the source-terminal pairs in Eq. (1). Likewise, computing optimal power flow and checking isolated loads or generators during the cascading failure simulation are possible improvements to DCLPFM.

Based on the numerical investigations, we conclude that the choice between ODBCM and DCLPFM for simulating cascading effects does not have significant impact in the average value of the loss measure, especially with random GMF. The conditional distribution of the risk metric is more sensitive to the uncertainty in the ground motion (compare second row with first row in Fig. 6) than to the choice of cascading effects model. Further investigations should consider more advanced cascading effect models, as well as multi-hazard scenarios (e.g., earthquake and tsunami).

Acknowledgement

This work has been sponsored by the research and development project RIESGOS (Grant No. 03G0876A-H) and RIESGOS 2.0 (Grant No. 03G0905A-J), both funded by the German Federal Ministry of Education and Research (BMBF) as part of the funding programme "BMBF CLIENT II International Partnerships for Sustainable Innovations".

The PyPSA power flow model was build by Juan Chaves-Santander and the GIS data of the consumer areas and simplified distribution lines by Angélica Soto-Calderón, both student assistants at the TU Munich.

References

Abedi, A., L. Gaudard, and F. Romerio (2019). Review of major approaches to analyze vulnerability in power system. *Reliab. Eng. Sys. Safe. 183*, 153–172.

Brandes, U. (2001). A faster algorithm for betweenness centrality. *J Math. Sociol. 25*(2), 163–177.

Brown, T., J. Hörsch, and D. Schlachtberger (2018). Python for power system analysis. *J. Open Res. Softw. 6*(1), 4.

CNE (2016). Energía Maps. Comisión Nacional de Energía (CNE), Chile. `energiamaps.cne.cl`.

Coordinador (2019). Infotécnica Sistema Eléctrico Nacional. Coordinador Eléctrico Nacional, Chile. `infotecnica.coordinador.cl`.

Cornell, C. A. (1968, 10). Engineering seismic risk analysis. *Bull. Seismol. Soc. Am. 58*(5), 1583–1606.

Crucitti, P., V. Latora, and M. Marchiori (2004). Model for cascading failures in complex networks. *Phys. Rev. E 69*, 045104.

CSN (2022). *Sismos Importantes y/o Destructivos (1570 a la fecha)*. Centro Sismológico Nacional, Universidad de Chile. `www.csn.uchile.cl/sismologia/grandes-terremotos-en-chile`.

Cupac, V., J. T. Lizier, and M. Prokopenko (2013). Comparing dynamics of cascading failures between network-centric and power flow models. *Int. J. Electr. Power Energy Syst. 49*, 369–379.

Douglas, J. (2021). *Ground Motion Prediction Equations 1964-2021*. Glasgow, UK: University of Strathclyde. `www.gmpe.org.uk`.

El-Hawary, M. (2008). *Introduction to Electrical Power Systems*. John Wiley Sons Ltd.

Farina, A., A. Graziano, F. Mariani, and F. Zirilli (2008). Probabilistic analysis of failures in power transmission networks and phase transitions: Study case of a high-voltage power transmission network. *J. Optim. Theory Appl. 139*(1), 171–199.

FEMA (2003). *HAZUS MH MR4 multi-hazard loss estimation methodology - Earthquake model*. Technical manual.

Ferrario, E., A. Poulos, J. C. de la Llera, A. Lorca, A. Oneto, and C. Magnere (2019). Representation and Modeling of the Chilean Electric Power Network for Seismic Resilience Analysis. In *Proc., 29th Int. Eur. Saf. Reliab. Conf. ESREL 2019*, pp. 3374 – 3381.

GEM (2022). *The OpenQuake-engine User Manual*. Global Earthquake Model (GEM). OpenQuake Manual for Engine, version 3.13.0.

Goh, K.-I., B. Kahng, and D. Kim (2001). Universal behavior of load distribution in scale-free networks. *Phys. Rev. Lett. 87*, 278701.

Hernández-Fajardo, I. and L. Dueñas-Osorio (2013). Probabilistic study of cascading failures in complex interdependent lifeline systems. *Reliab. Eng. Sys. Safe. 111*, 260 – 272.

Hussain, E., J. R. Elliott, V. Silva, M. Vilar-Vega, and D. Kane (2020). Contrasting seismic risk for Santiago, Chile, from near-field and distant earthquake sources. *Nat. Hazards Earth Syst. Sci. 20*(5), 1533–1555.

INE (2017). Servicio de mapas del censo 2017. Instituto Nacional de Estadísticas, Chile. `www.censo2017.cl/servicio-de-mapas`.

Jayaram, N. and J. W. Baker (2009). Correlation model for spatially distributed ground-motion intensities. *Earthq. Eng. Struc. D. 38*(15), 1687–1708.

Jayaram, N. and J. W. Baker (2010). Efficient sampling and data reduction techniques for probabilistic seismic lifeline risk assessment. *Earthq. Eng. Struc. D. 39*(10), 1109 – 1131.

Moehle, J. and G. Deierlein (2004). A framework methodology for performance-based earthquake engineering. In *Proc., 13th World Conf. on Earthq. Eng. (13WCEE)*, pp. 679.

Montalva, G. A., N. Bastías, and A. Rodríguez-Marek (2017). Ground Motion Prediction Equation for the Chilean Subduction Zone. *Bull. Seismol. Soc. Am. 107*(2), 901–911.

Ouyang, M. (2013). Comparisons of purely topological model, betweenness based model and direct current power flow model to analyze power grid vulnerability. *Chaos 23*(2), 023114.

Pitilakis, K., H. Crowley, and A. Kaynia (Eds.) (2014). *SYNER-G: Typology Definition and Fragility Functions for Physical Elements at Seismic Risk*. Dodrecht, Netherlands: Springer.

Poljanšek, K., F. Bono, and E. Gutiérrez (2011). Seismic risk assessment of interdependent critical infrastructure systems: The case of European gas and electricity networks. *Earthq. Eng. Struc. D. 41*(1), 61–79.

Rosero-Velásquez, H. and D. Straub (2022). Selection of representative natural hazard scenarios for engineering systems. Manuscript submitted for publication. Preprint at `www.cee.ed.tum.de/era/publications`.

Tang, A. and J. M. Eidinger (Eds.) (2006). *Chile earthquake of 2010: Lifeline performance*. Number 36 in Technical Council on Lifeline Earthquake Engineering Monographs. Reston, Virginia, USA: American Society of Civil Engineers.

Wang, M. and T. Takada (2005). Macrospatial correlation model of seismic ground motions. *Earthq. Spectra 21*(4), 1137–1156.

Yang, T. Y., J. Moehle, B. Stojadinovic, and A. D. Kiureghian (2009). Seismic performance evaluation of facilities: Methodology and implementation. *J. Struct. Eng. 135*(10), 1146–1154.